Thermodynamics of Calmodulin Trapping by Ca^{2+}/Calmodulin-Dependent Protein Kinase II: Subpicomolar K_d Determined Using Competition Titration Calorimetry

Joyce K. Y. Tse,[‡] Anthony M. Giannetti,[§] and J. Michael Bradshaw*,[‡]

Departments of Biochemical Pharmacology and Biophysics and Crystallography, Roche Palo Alto LLC, 3431 Hillview Avenue, Palo Alto, California 94304

Received January 3, 2007; Revised Manuscript Received February 2, 2007

ABSTRACT: Calmodulin (CaM) trapping by Ca^{2+}/calmodulin-dependent protein kinase II (CaMKII) is a phenomenon whereby the affinity of CaM for CaMKII increases >1000-fold following CaMKII autophosphorylation. The molecular basis of this effect is not entirely understood. Binding of CaM to the phosphorylated and the unphosphorylated states of CaMKII is well mimicked by the interaction of CaM with two different length peptides taken from the CaM-binding region of CaMKII, peptides we refer to as the long and intermediate peptides. To better understand the conformational change accompanying CaM trapping, we have used isothermal titration calorimetry (ITC) to compare the binding thermodynamics of CaM to these peptides as well as to a shorter CaMKII-based peptide. Calorimetric analysis revealed that the enthalpy, rather than the entropy, distinguished binding of these three peptides. Furthermore, the heat capacity change was found to be similar for the long and intermediate peptides but smaller in magnitude for the short peptide. Direct titration of CaM with peptide provided the K_d value for the short peptide (K_d = 5.9 ± 2.4 μM), but a novel, two-phased competitive binding strategy was necessary to ascertain the affinities of the intermediate (K_d = 0.17 ± 0.06 nM) and long (K_d = 0.07 ± 0.04 pM) peptides. To our knowledge, the K_d for the long peptide is the most potent measured to date using ITC. Together, the findings reported here support a model whereby the final conformational change accompanying CaM trapping buries little additional surface area but does involve formation of new hydrogen bonds and van der Waals contacts that contribute to formation of the high-affinity, CaM-trapped state.

Ca^{2+}/calmodulin-dependent protein kinase II (CaMKII)[1] is a multifunctional serine/threonine kinase that plays an important role in many physiological functions including learning and memory in the brain (*1*−*6*). Autophosphorylation of CaMKII at residue Thr 286 (α-isoform) is essential to its function (*7*, *8*). One consequence of Thr 286 autophosphorylation is a >1000-fold decrease in the rate of dissociation of calmodulin (CaM) from CaMKII, a phenomenon referred to as "CaM trapping" (*9*). While CaM trapping by CaMKII is believed to profoundly impact the information flow in many Ca^{2+}-mediated signaling networks (*10*, *11*), the molecular basis of this phenomenon remains incompletely understood.

CaM trapping was originally discovered as a dramatic decrease in the dissociation rate of fluorescently labeled CaM following CaMKII autophosphorylation (*9*). Specifically, the $t_{1/2}$ in the presence of calcium increases from ∼1 s to >2 h following ATP addition. Thr 286 autophosphorylation is essential to the effect since a CaMKII T286A mutant demonstrates reduced trapping (*9*). The first studies to probe the molecular basis of CaM trapping employed peptides based on the CaM-binding region of CaMKII (*12*, *13*). In these works, it was found that a peptide based on the minimum CaM-binding sequence of CaMKII (which we refer to as the intermediate peptide) displays a dissociation rate similar to unphosphorylated CaMKII; in contrast, a longer peptide that had been used for the CaM−CaMKII peptide crystal structure (which we call the long peptide) dissociates similarly to phosphorylated CaMKII (for peptide sequences, see Figure 1). On the basis of these findings, it was proposed that the long and intermediate peptides provide a good model for the interaction of CaM with the phosphorylated and unphosphorylated states of CaMKII, respectively (*12*). Specifically, a molecular model for CaM trapping was suggested whereby new contacts form between CaM and residues 293−295 of CaMKII following Thr 286 autophosphorylation (*13*). The importance of Phe 293 and Asn 294 for CaM trapping was subsequently confirmed in studies that used mutagenesis to investigate CaM trapping in full-length CaMKII (*14*, *15*).

While strong evidence suggests that CaM trapping involves formation of new contacts between CaM and residues 293−295 of CaMKII, the conformation adopted by CaM after binding CaMKII but before autophosphorylation remains unclear. CaM has recently been demonstrated to show considerable plasticity in its interaction with targets (*16*),

* To whom correspondence should be addressed. Tel: 650-855-5592. Fax: 650-855-6078. E-mail: Michael.bradshaw@roche.com.

[‡] Department of Biochemical Pharmacology, Roche Palo Alto LLC.

[§] Department of Biophysics and Crystallography, Roche Palo Alto LLC.

[1] Abbreviations: CaMKII, Ca^{2+}/calmodulin-dependent protein kinase II; CaM, calmodulin; ITC, isothermal titration calorimetry; IPTG, isopropyl β-D-thiogalactopyranoside; ASA, solvent-accessible surface area; smMLCK, smooth muscle myosin light chain kinase; CaMKI, CaM kinase I; BSA, bovine serum albumin; IADANS, *N*-(iodoacetyl)-*N*′-(5-sulfo-1-naphthyl)ethylenediamine; FRET, fluorescence resonance energy transfer.

10.1021/bi700013y CCC: $37.00
Published on Web 03/13/2007

Peptide Name	CaMKII Residues	Peptide Sequence
Long	CKII(291-312)	Ac-KKFNARRKLKGAILTTMLATRN-NH_2
Intermediate	CKII(296-312)	Ac-RRKLKGAILTTMLATRN-NH_2
Short	CKII(300-312)	Ac-KGAILTTMLATRN-NH_2

FIGURE 1: Peptides used in this study. Shown are the name of the peptide (left), the residues of αCaMKII that correspond to this peptide (center), and the peptide sequence (right).

suggesting that the conformations adopted by CaM before and after Thr 286 phosphorylation may be different. A study with dual-labeled fluorescent CaM supports this notion in that CaM adopts a "semicompact" conformation upon binding CaMKII that becomes fully compact following autophosphorylation (*17*).

CaM trapping by CaMKII has not yet been investigated using isothermal titration calorimetry (ITC), but ascertaining the thermodynamics parameters (K_d, ΔG, ΔH, $T\Delta S$, ΔC_p) for binding of CaMKII-based peptides to CaM would provide additional information about the conformational change accompanying CaM trapping. Specifically, K_d (and hence ΔG) reports on the affinity of the interaction, the binding enthalpy (ΔH) provides a measure of the extent of hydrogen bonds and van der Waals interactions formed upon binding, the binding entropy ($T\Delta S$) reports on the change in translational, rotational, and vibrational degrees of freedom upon binding as well as changes in desolvation, and the heat capacity change (ΔC_p) reports on the degree of surface area buried. A limitation of using ITC to study CaM binding is that tight binding interactions (i.e., $K_d < 1$ nM) cannot be determined directly due to the sensitivity limit of the calorimeter. However, it is not widely appreciated that this difficulty can be overcome if a competitive binding approach is employed. Performing ITC experiments with a strong ligand in the presence of a weaker ligand of known K_d will weaken the apparent binding affinity of the strong ligand, permitting accurate determination of its K_d (see Appendix).

In this work, we employed an ITC-based competition approach to determine the binding affinity and other thermodynamic parameters for CaM binding to three peptides based on the CaM-binding region of CaMKII. We obtained a complete thermodynamic characterization of the long, intermediate, and short peptides in order to better understand the structural transition that takes place upon CaM trapping by CaMKII. To accomplish this, a two-step competition strategy was utilized where the short peptide was first used as a competitor for the intermediate peptide, and subsequently the intermediate peptide was used as a competitor for the long peptide. Using this approach, a remarkably potent K_d for CaM binding to the long peptide of 0.07 ± 0.04 pM was determined. Overall, the thermodynamic characterization of these peptides has provided greater insight into the molecular mechanism of CaM trapping by CaMKII.

MATERIALS AND METHODS

Protein Expression and Purification. The CaM gene was previously cloned into a pCR2 vector (Invitrogen) for expression in *Escherichia coli* BL21(DE3) cells (Invitrogen) (*14*). *E. coli* growth and protein expression were conducted in a single day. Starting from an isolated bacterial colony, *E. coli* cells were incubated in LB with 1 mg/mL ampicillin at 37 °C. The culture volume was progressively increased from 5 mL to 200 mL to 1 L when an OD = 0.5 was attained. CaM expression was induced in the 1 L culture at OD = 0.5 for 3 h with 1 mM isopropyl β-D-thiogalactopyranoside (IPTG). Following induction, cells were harvested and stored at −20 °C.

Pellets were resuspended in 50 mM Tris, pH 7.5, and 1 mM EDTA, with protease inhibitor cocktail (Sigma), and sonicated using a probe sonicator. Following centrifugation at 30000*g* for 25 min, the supernatant was heated to 70 °C while being continuously stirred. The material was centrifuged at 30000*g* for an additional 25 min, and the supernatant was again collected. Two 10 mL columns of phenyl-Sepharose CL-4B (Sigma) were then equilibrated with 100 mL of buffer: column 1 with 50 mM Tris, pH 7.5, and 0.5 mM EGTA and column 2 with 50 mM Tris, pH 7.5, and 2 mM $CaCl_2$. The supernatant was applied to column 1, and the flow-through was retained. $CaCl_2$ was added to the flow-through to a final concentration of 10 mM, and the material was applied to column 2. Column 2 was first washed with 25 mL of 50 mM Tris, pH 7.5, and 2 mM $CaCl_2$, then with 25 mL of 50 mM Tris, pH 7.5, 2 mM $CaCl_2$, and 0.5 M NaCl, and finally with 25 mL of 50 mM Tris, pH 7.5, and 2 mM $CaCl_2$. CaM was eluted in 3 mL fractions with 50 mM Tris, pH 7.5, and 10 mM EGTA. Following evaluation with SDS−PAGE, the protein was extensively dialyzed into 20 mM Hepes, pH 7.15, 100 mM NaCl, and 2 mM $CaCl_2$ and stored in this buffer at −20 °C. The concentration of CaM was evaluated using extinction coefficients of 2900 M^{-1} cm^{-1} ($-Ca^{2+}$) or 3100 M^{-1} cm^{-1} ($+Ca^{2+}$) at 276 nm (*18*).

CaMKII Peptides. Peptides were based on the CaM-binding region of rat α-CaMKII. Two separate batches of each peptide were synthesized, the first from Quality Controlled Biochemicals (Hopkinton, MA) and the second from Roche (Nutley, NJ). Each batch behaved identically in ITC titrations. The employed peptide sequences are shown in Figure 1. Another peptide, CaMKII(296−304), was also examined in ITC experiments and found not to bind to CaM; the sequence of CaMKII(296−304) was Ac-RRKLKGAIL-NH_2. Peptides were directly dissolved into the ITC buffer of 20 mM Hepes, pH 7.15, 100 mM NaCl, and 2 mM $CaCl_2$ prior to calorimetric titrations. Peptide concentration was preliminarily determined by mass and then confirmed using the stoichiometry of binding of calorimetric titrations.

Isothermal Titration Calorimetry. ITC experiments were performed with a VP-ITC system obtained from Microcal, Inc. (Northampton, MA). Solutions were degassed for 10 min prior to experiments. The standard ITC conditions were 20 mM Hepes, pH 7.15, 100 mM NaCl, and 2 mM $CaCl_2$ at 25 °C. Experiments that employed cacodylate or imidazole buffer instead of Hepes also contained a concentration of 20 mM. The heat of ionization (ΔH_{ion}) of each of these buffers at 25 °C was the following: cacodylate, $\Delta H_{ion} = -0.56$ kcal/mol; Hepes, $\Delta H_{ion} = 5.00$ kcal/mol; imidazole, $\Delta H_{ion} = 8.76$ kcal/mol (*19*). For a typical titration of CaM with CaMKII peptide, 5−50 μM [CaM] was placed in the reaction cell while a solution of 100 μM to 1 mM CaMKII peptide was placed in the ITC syringe. Five microliters of peptide was then injected into the reaction cell at 3.5−5 min intervals.

For competition experiments, the competing peptide was dissolved to an equal concentration in both the reaction cell and the syringe to ensure that its concentration did not change

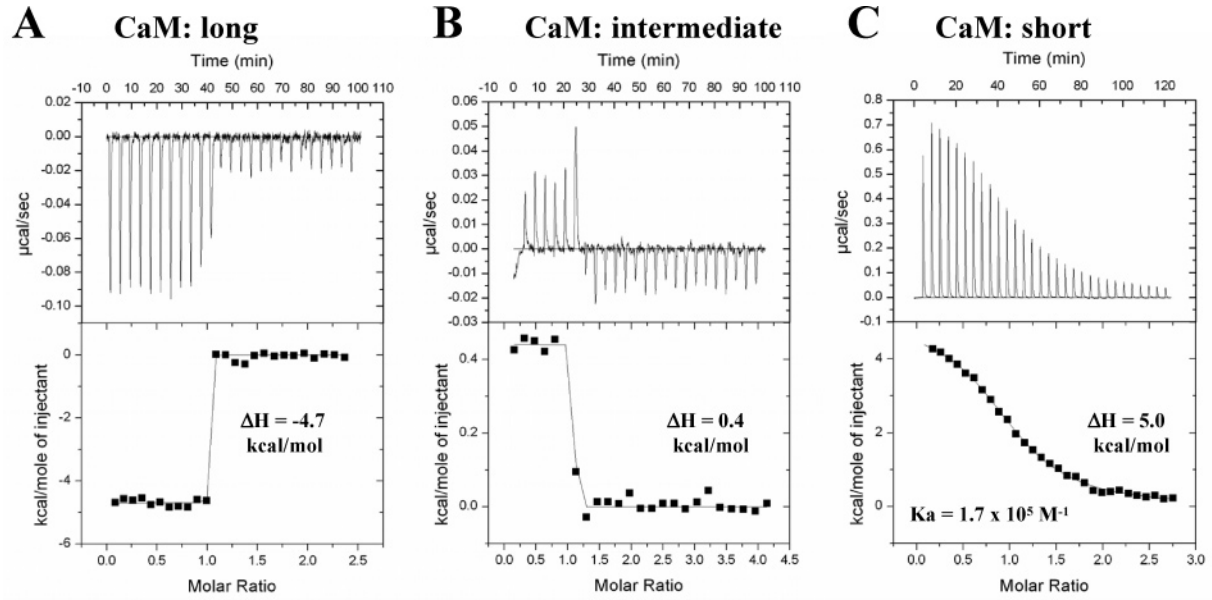

FIGURE 2: Calorimetric data for binding of CaM to CaMKII-based peptides. Shown is binding of long (A), intermediate (B), and short (C) peptides. The top panels show the raw power output (μcal/s) per unit time (min). The bottom panels show the integrated data (kcal/mol per injection versus molar ratio of peptide to CaM). These data are obtained from the raw power output as the area underneath each peak, which is then corrected for baseline heat injections. The solid line through each data set represents the nonlinear least-squares best fit of the data to a single-site binding model as described in Materials and Methods. These titrations were performed in 20 mM Hepes, pH 7.15, 100 mM NaCl, and 2 mM $CaCl_2$ at 25 °C. The ΔH and K_a values (if applicable) of the individual titrations are shown in the bottom panels.

during the course of the experiment. For titration of CaM with the intermediate peptide, the concentration of the competing short peptide varied from 120 to 700 μM. For titration of CaM with the long peptide, the concentration of competing intermediate peptide varied from 1 to 3 mM. A sophisticated method for analysis of competitive displacement data using ITC has been developed (*20*), but the experimental design employed here does not require sophisticated analysis. This is because here the competitive ligand was placed at equal concentration in both the syringe and the reaction cell, causing the concentration of competitor to remain constant throughout the experiment. This strategy allowed the data to be analyzed using standard ITC methods.

Analysis of Calorimetric Data. ITC data were collected automatically using the Origin software. Data were corrected for heats of injection by subtracting the basal heat that remained following saturation prior to further analysis. Data were fit using a nonlinear least-squares algorithm (Marquardt method) packaged with the Origin software provided with the VP-ITC system. All data fit well to a single-site binding model which provided the stoichiometry (n), association constant (K_a), and enthalpy (ΔH) of binding. The value of n for all experiments was found to be between 0.75 and 1.2. The values of K_a and ΔH were used to calculate the change in free energy (ΔG) and entropy (ΔS) of binding using the expressions:

$$\Delta G = -RT \ln K_a \quad (1)$$

$$\Delta G = \Delta H - T\Delta S \quad (2)$$

Calculation of Solvent-Accessible Surface Area. Calculations of solvent-accessible surface area were performed using the Web-accessible program GETAREA (*21*). This program separates the accessible surface area into polar and nonpolar components. A probe radius of 1.4 Å was employed. To make these calculations, the crystal structures of Ca^{2+}/CaM (*22*) and Ca^{2+}/CaM bound to the long peptide (*23*) were used as models for the conformation of CaM in its peptide-free and peptide-bound states, respectively. The long, intermediate, and short peptides were each modeled using the conformation of the long peptide (minus the appropriate residues) in the Ca^{2+}/CaM−long peptide structure. The change in solvent-accessible surface area (ASA) was calculated using the formula:

$$\Delta ASA = ASA_{CaM+peptide} - (ASA_{CaM} + ASA_{peptide}) \quad (3)$$

Evaluation of the calculated heat capacity change (ΔC_{pcalc}) based on the change in surface area was performed using the expression proposed by Spolar and Record (*24*):

$$\Delta C_{pcalc} = 0.32(\Delta ASA_{npol}) - 0.14(\Delta ASA_{pol}) \quad (4)$$

Here, ΔASA_{npol} and ΔASA_{pol} represent the change in nonpolar and polar surface area upon binding, respectively.

RESULTS

Thermodynamics of CaM Binding to the Long, Intermediate, and Short Peptides. To better understand the different conformations adopted by CaM when bound to different CaMKII peptides, the thermodynamics of CaM binding to the long, intermediate, and short peptides were investigated using ITC. Representative titrations at 25 °C are shown in Figure 2. For the long peptide, binding was found to be exothermic ($\Delta H = -4.7$ kcal/mol) but too potent for K_a to be determined (Figure 2A). The intermediate peptide displayed a very small, endothermic signal upon binding, and like the long peptide, the interaction was too tight for K_a to be evaluated (Figure 2B). Binding of the short peptide was endothermic and weaker such that an association constant of $K_a = 1.7 \pm 0.7 \times 10^5$ M^{-1} ($K_d = 5.9 \pm 2.4$ μM) was ascertained (Figure 2C).

Table 1: Titration Calorimetry Data for CaM Binding to CaMKII-Based Peptides[a]

peptide	buffer	K_a (M^{-1})	ΔH (kcal/mol)
long	Hepes		-6.1 ± 0.8
intermediate	Hepes		0.5 ± 0.2
short	Hepes	$1.7 \pm 0.7 \times 10^5$	5.0 ± 0.7
long	cacodylate		-7.0 ± 1.0
intermediate	cacodylate		-1.2 ± 0.6
short	cacodylate	$1.3 \pm 0.4 \times 10^5$	4.0 ± 0.7
long	imidazole		-5.4 ± 0.9
intermediate	imidazole		2.0 ± 0.9
short	imidazole	$1.8 \pm 0.9 \times 10^5$	6.7 ± 1.0

[a] All experiments were performed at 25 °C in 20 mM buffer, pH 7.15, 100 mM NaCl, and 2 mM $CaCl_2$. Errors represent the standard deviation of multiple experiments. The ΔH_{ion} values for Hepes, cacodylate, and imidazole buffers are 5.0, −0.56, and 8.76 kcal/mol, respectively.

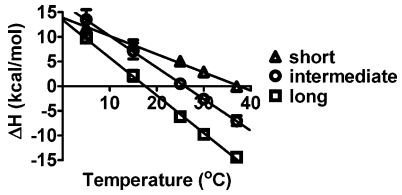

FIGURE 3: Enthalpies of CaM binding to CaMKII-based peptides as a function of temperature. Shown are ΔH values (kcal/mol) for the short (open triangles), intermediate (open circles), and long (open squares) peptides. The solid line represents the linear least-squares best fit to the data. The ΔC_p values are the following: long peptide = -0.79 ± 0.03 kcal mol^{-1} deg^{-1}; intermediate peptide = -0.64 ± 0.04 kcal mol^{-1} deg^{-1}; short peptide = -0.34 ± 0.04 kcal mol^{-1} deg^{-1}. Error bars represent the standard deviation of multiple experiments. The solution conditions were 20 mM Hepes, pH 7.15, 100 mM NaCl, and 2 mM $CaCl_2$.

The observed enthalpy (ΔH) in these ITC titrations could reflect the composite heat of multiple processes including the enthalpy of the binding process itself corrected for buffer effects (ΔH_{corr}) as well as the enthalpy of ionization (ΔH_{ion}) of the employed buffer. These values are related by the expression:

$$\Delta H = \Delta H_{corr} + n\Delta H_{ion} \quad (5)$$

where n is the number of protons exchanged upon binding. In order to deconvolute ΔH_{corr} (the enthalpy of interest) from ΔH_{ion}, ITC experiments were performed in different buffers with different values of ΔH_{ion}. In these experiments, a dependence of ΔH on the employed buffer would reflect a contribution from protonation to ΔH (*25*, *26*). Table 1 shows the results of ITC experiments with the long, intermediate, and short peptides in Hepes, cacodylate, and imidazole buffers. ΔH was found to display minimal dependence on the employed buffer for all peptides (Table 1), indicating little contribution to ΔH from proton exchange. Hence, ΔH is a good reflection of ΔH_{corr} for all peptides. Previous studies have also found that CaM−peptide interactions demonstrate little proton exchange near pH 7.0 (*27*).

To determine the heat capacity change (ΔC_p) for each peptide, the temperature dependence of binding was examined. Titrations were performed at 5, 15, 25, 30, and 37 °C. Plotting ΔH as a function of temperature revealed a linear dependence whose slope provided ΔC_p (Figure 3). The long peptide was found to have a ΔC_p of -0.79 ± 0.03 kcal mol^{-1} deg^{-1} while ΔC_p for the intermediate peptide was -0.64 ± 0.04 kcal mol^{-1} deg^{-1}. The ΔC_p for the short peptide was smaller at -0.34 ± 0.04 kcal mol^{-1} deg^{-1}. Since ΔC_p is believed to reflect the degree of surface area buried upon binding (*24*), the long peptide appears to bury a similar surface area as the intermediate peptide but more area than the short peptide.

When structural information is available, it is customary to quantitatively compare the experimental ΔC_p (ΔC_{pexp}) with predictions of ΔC_p (ΔC_{pcalc}) from the polar and nonpolar surface area buried upon binding (*24*, *28*). Calculations of solvent-accessible surface area (see Materials and Methods) determined that ΔC_{pcalc} reproduced ΔC_{pexp} for the long and intermediate peptides but overestimated ΔC_{pexp} for the short peptide (Table 2). This suggests that the surface area buried in solution when CaM binds the long and intermediate peptides resembles that buried in the CaM−long peptide crystal structure, but CaM buries less surface area when binding to the short peptide (see Discussion).

Several other ITC experiments were performed to further characterize CaM−CaMKII peptide interactions. To further validate the CaMKII peptide binding parameters, we reversed the order of the ITC titration by placing CaM in the syringe and the intermediate peptide in the reaction cell. This experimental setup generated a stoichiometric binding curve with a ΔH of -7.7 ± 0.3 kcal/mol at 37 °C, very similar to the standard arrangement with CaM in the reaction cell (ΔH of -6.4 ± 0.4 at 37 °C). Continuing to study the CaM^- intermediate peptide interaction at 37 °C, it was examined whether varying the NaCl concentration affected the thermodynamic parameters. A titration performed with 500 mM rather than 100 mM [NaCl] gave a ΔH of -5.8 ± 0.6 kcal/mol, indicating that [NaCl] has little effect on the binding enthalpy. Varying [NaCl] also had little impact for binding of CaM to a peptide based on smooth muscle myosin light chain kinase (smMLCK) (*27*). Since Mg^{2+} is known to compete with Ca^{2+} for binding to CaM, we also explored if ITC titrations performed in $MgCl_2$ would perturb CaM−CaMKII peptide binding. However, little difference was observed between titrations performed with and without 50 mM $MgCl_2$ ($\Delta H_{+Mg^{2+}} = -6.1 \pm 0.4$ kcal/mol). We also found no difference in binding of CaM to the intermediate peptide if the solution pH was 7.5 rather than 7.15. Finally, it was determined that Ca^{2+} is required for CaM−intermediate peptide interaction because an experiment performed in 5 mM EGTA did not show binding; on the basis of this experiment, we estimate that the K_d for this interaction is greater than 100 μM. Ca^{2+} was also found to be necessary for binding of the long and short peptides to CaM.

Competitive Binding Experiments for CaM−CaMKII Peptide Interactions. Having established the ΔH and ΔC_p values for each peptide, we sought the intrinsic K_a for binding of the long and intermediate peptides in order to calculate the free energy (ΔG) and entropy (ΔS) for each peptide. Since the intrinsic K_a could not be determined by direct titration, a competition strategy was used. In these experiments, binding of CaM to the peptide with unknown K_a was studied in the presence of a competing, weaker peptide with known K_a. This decreased the observed association constant (K_{obs}) so that it was measurable, which allowed the intrinsic K_a to be calculated. The equations employed to calculate the intrinsic K_a and ΔH values for the long and intermediate peptides are derived in the Appendix.

Table 2: Change in Surface Area upon Peptide Binding to CaM and Calculated Heat Capacity Change

peptide	ΔASA_{tot}[a]	ΔASA_{np}[a] (Å^2)	ΔASA_{p}[a] (Å^2)	ΔC_{pcalc}[b] (kcal mol^{-1} deg^{-1})	ΔC_{pexp}[c] (kcal mol^{-1} deg^{-1})
long	3832	2871	961	-0.78 ± 0.12	-0.79 ± 0.03
intermediate	3649	2697	952	-0.73 ± 0.11	-0.64 ± 0.04
short	2971[a]	2236	735	-0.61 ± 0.10	-0.34 ± 0.03

[a] Calculated from eq 3 (see Materials and Methods). [b] Calculated from eq 4 (see Materials and Methods). [c] Determined experimentally as described in the text.

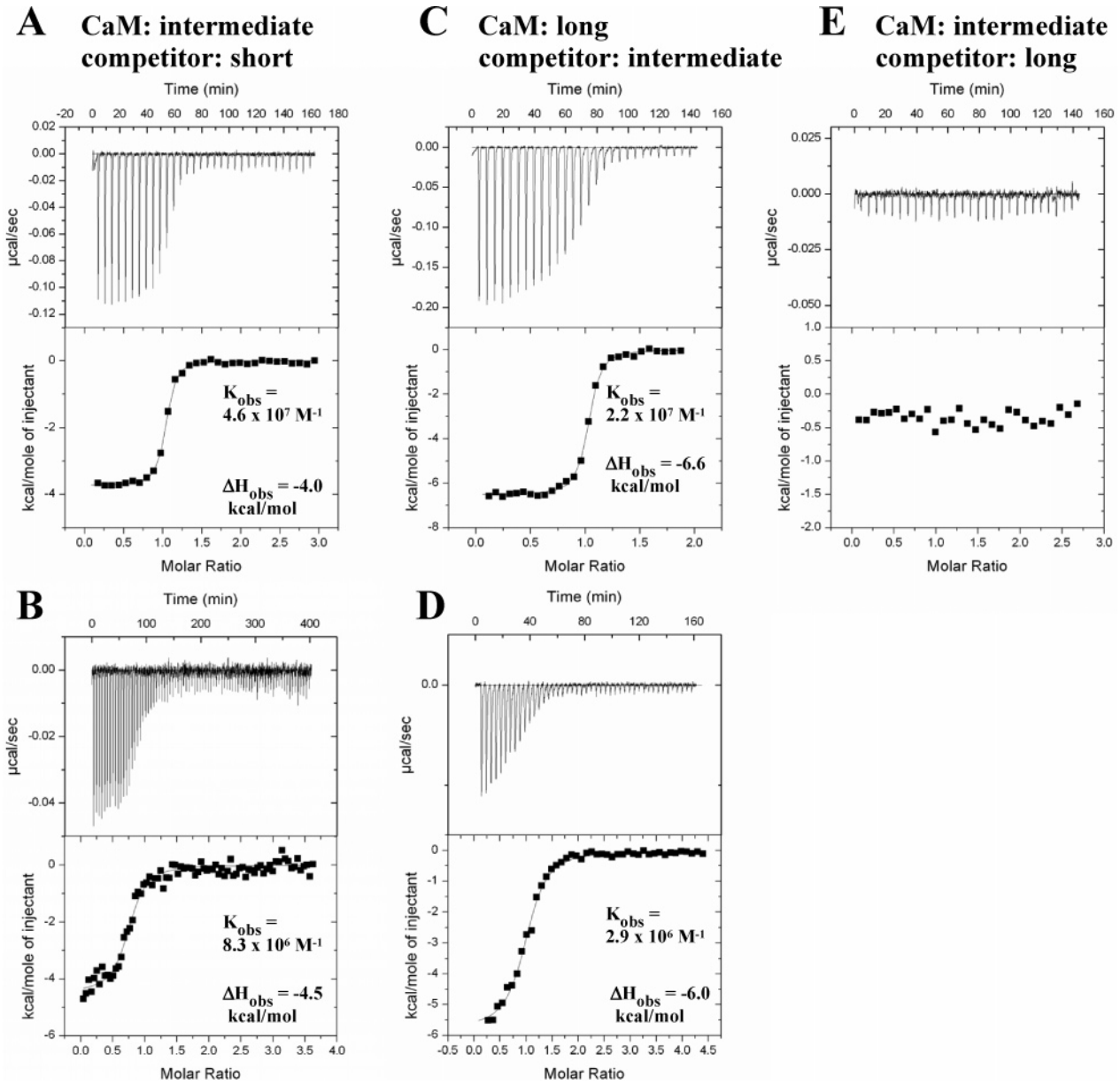

FIGURE 4: Calorimetric data for competition binding experiments. Shown are binding of the intermediate peptide using the short peptide as a competitor at 1 mM (A) or at 3 mM (B), binding of the long peptide using the intermediate peptide as a competitor at 150 μM (C) or at 700 μM (D), and binding of the intermediate peptide using the long peptide as a competitor at 20 μM (E). The top panels show the raw power output (μcal/s) per unit time (min). The bottom panels show the integrated data (kcal/mol per injection versus molar ratio of peptide to CaM). The *c* values for each experiment are given in Table 3. These titrations were performed in 20 mM Hepes, pH 7.15, 100 mM NaCl, and 2 mM $CaCl_2$ at 25 °C. The observed ΔH and K_a values (if applicable) of the individual titrations are shown in the bottom panels.

Since K_a of the short peptide had previously been established through direct titration, it was chosen to be the low-affinity competitor in titrations of CaM with the intermediate peptide. Initial titrations of the intermediate peptide at concentrations of the short peptide that were less than 500 μM failed to provide conditions to evaluate K_{obs} since binding remained very tight (data not shown). However, a subsequent experiment using 1 mM short peptide produced a titration curve that could be analyzed (Figure 4A). The K_{obs} for this titration was determined to be $4.6 \pm 0.8 \times 10^7$ M^{-1} (Table 3). A subsequent titration using 3 mM short peptide further reduced K_{obs} to $8.3 \pm 1.4 \times 10^6$ M^{-1} (Figure 4B, Table 3). Using eq 11 in the Appendix, the intrinsic K_a for intermediate peptide binding to CaM was calculated for

Table 3: Data Parameters for ITC Competition Experiments[a]

titrated peptide	competing peptide	[competing peptide] (μM)	K_{obs}[b] (M^{-1})	ΔH_{obs}[b] (kcal/mol)	$K_{a\ calc}$[c] (M^{-1})	ΔH_{calc}[d] (kcal/mol)	ΔH_{exp}[e] (kcal/mol)	c[f]
intermediate	short	1000	$4.6 \pm 0.8 \times 10^7$	-4.0 ± 0.1	$7.8 \pm 1.9 \times 10^9$	1.0 ± 0.2	0.5 ± 0.2	276
intermediate	short	3000	$8.3 \pm 1.4 \times 10^6$	-4.5 ± 0.1	$4.2 \pm 1.6 \times 10^9$	0.5 ± 0.2	0.5 ± 0.2	37
long	intermediate	150	$2.2 \pm 0.3 \times 10^7$	-6.6 ± 0.1	$2.0 \pm 0.4 \times 10^{13}$	-6.1 ± 0.2	-6.1 ± 0.8	324
long	intermediate	700	$2.9 \pm 0.4 \times 10^6$	-6.0 ± 0.2	$1.2 \pm 0.2 \times 10^{13}$	-5.5 ± 0.3	-6.1 ± 0.8	22

[a] All experiments were performed at 25 °C in 20 mM Hepes, pH 7.15, 100 mM NaCl, and 2 mM $CaCl_2$. Errors represent the standard error of the fitting procedure or else were calculated using standard error propagation. [b] Determined experimentally as described in the text. [c] Calculated using eq 11. [d] Calculated using eq 15. [e] Determined experimentally as described in the text (see Table 1). [f] Calculated using eq 6.

both experiments. The calculated K_a values agreed within a factor of 2 from these independent titrations (Table 3) and provided a mean intrinsic K_a for the intermediate peptide of $6.0 \pm 2.0 \times 10^9$ M^{-1} ($K_d = 0.17 \pm 0.06$ nM).

Having established the binding affinity of the intermediate peptide, this peptide was used as the low-affinity competitor in titrations of CaM with the long peptide. Initially, 120 μM intermediate peptide was employed as the competitor. Here, a K_{obs} of $2.7 \pm 0.7 \times 10^7$ M^{-1} was determined (Figure 4C, Table 3). Subsequently, 700 μM intermediate peptide was used to compete with binding. As expected, K_{obs} was further reduced under these conditions to a value of $2.8 \pm 0.9 \times 10^6$ M^{-1} (Figure 4D, Table 3). The intrinsic K_a value for the long peptide calculated using eq 11 was nearly identical for these two experiments (Table 3), giving a mean intrinsic K_a of $1.5 \pm 1.1 \times 10^{13}$ M^{-1}. This corresponds to a K_d of 0.07 $\pm$ 0.04 pM.

How do we know if the K_{obs} values from the competition experiments described above are within a range where they can be measured accurately? Wiseman et al. have reported that K_{obs} can be accurately determined from ITC experiments if the c value of the experiment is between 1 and 1000, with the optimal range being 10 to 100 (*29*). Here, the c value is defined as the product of the macromolecule concentration (here, CaM) and K_{obs}:

$$c = [\mathrm{CaM}]K_{obs} \quad (6)$$

We calculated that the c values were between 20 and 400 for all competition binding experiments (Table 3). This corroborates that K_{obs} in these experiments is accurate.

The intrinsic ΔH for binding of the long and intermediate peptides had already been determined from direct titration of each peptide with CaM (see Figure 2 and Table 1). However, the ΔH_{obs} determined in the competition experiments can also be used as an independent method to calculate the intrinsic ΔH for each peptide (see eq 15 in the Appendix). How closely do these two independent ways of determining ΔH correspond? Table 3 reveals that for both peptides the ΔH calculated from competition experiments agrees within 0.5 kcal/mol to the ΔH that was measured by direct titration, validating the use of competition binding to determine K_a for the long and intermediate peptides.

To further validate the competition approach, a control experiment was performed where the long peptide was used as the competitor and CaM was titrated with the intermediate peptide. As expected, binding of the intermediate peptide is completely blocked under these conditions (Figure 4E).

Table 4 compares the K_d for the long and intermediate peptides measured here with estimated K_d values for the same peptides obtained in a previous study (*12*) by examining the kinetics of association and dissociation of a fluorescently labeled CaM. While the values are similar, the potency measured here is 3−10-fold greater. This modest discrepancy is not unexpected given the different versions of CaM used in these studies and the different experimental assay conditions (Table 4). Nonetheless, the ITC competition experiments described here have revealed that the CaM−long peptide interaction is even more potent than had previously been believed.

Table 4: Comparison of CaM-peptide Binding Parameters Determined by ITC and Fluorescence Spectroscopy

	ITC[a]	fluorescence[b]		
peptide	K_d (nM)	K_d (nM)	k_{on} (M^{-1} s^{-1})	k_{off} (s^{-1})
long	0.00007 ± 0.00004	0.0002	3.2×10^8	0.00007
intermediate	0.17 ± 0.06	2	1.3×10^8	0.26

[a] Parameters determined in this work in 20 mM Hepes, pH 7.15, 100 mM NaCl, and 2 mM $CaCl_2$. [b] Parameters determined in 25 mM MOPS, pH 7.0, 150 mM KCl, 0.1 mg/mL BSA, and 0.5 mM $CaCl_2$ with IADANS-labeled CaM as described in ref *12*.

DISCUSSION

In this work, the thermodynamic basis of CaM trapping was investigated by studying the binding of CaM to three peptides based on the CaM-binding region of CaMKII. The thermodynamic parameters calculated from ITC data for the long, intermediate, and short peptides are shown in Table 5 and Figure 5. Using a competitive binding approach, it was revealed that N-terminal peptide residues profoundly affect CaM binding; the long peptide binds 2500-fold more potently than the intermediate peptide and 100000000-fold more potently than the short peptide. These values correspond to a difference in ΔG of 4.6 ± 0.6 kcal/mol and 10.8 ± 0.5 kcal/mol, respectively. The difference in peptide potency at 25 °C is due entirely to differences in ΔH since $T\Delta S$ is quite similar for all peptides (Figure 5). Specifically, $T\Delta S$ makes a favorable contribution to binding for all peptides ($T\Delta S \sim$ 12 kcal/mol), but the contribution of ΔH is unfavorable for the short peptide, neutral for the intermediate peptide, and favorable for the long peptide. Furthermore, ΔC_p values for the long and intermediate peptides are similar but larger in magnitude than for the short peptide (Table 4).

What do the thermodynamics suggest about the conformation of CaM when bound to each peptide? Since ΔC_p is widely believed to reflect the degree of surface area buried upon binding, the data suggest that the long peptide buries only slightly more surface area than the intermediate peptide but significantly more than the short peptide. A recent investigation using ITC to study CaM binding to eight diverse targets noted that ΔC_p values for CaM−peptide interactions

Table 5: Thermodynamic Parameters of CaM Binding to CaMKII-Based Peptides[a]

peptide	K_a[b] (M^{-1})	K_d[c] (nM)	ΔG[c] (kcal/mol)	ΔH[b] (kcal/mol)	$T\Delta S$[c] (kcal/mol)	ΔC_p[d] (kcal mol^{-1} deg^{-1})
long	$1.5 \pm 1.1 \times 10^{13}$	0.00007 ± 0.00004	-17.9 ± 0.5	-6.1 ± 0.8	11.8 ± 0.9	-0.79 ± 0.03
intermediate	$6.0 \pm 2.0 \times 10^{9}$	0.17 ± 0.06	-13.3 ± 0.4	0.5 ± 0.2	13.8 ± 0.6	-0.64 ± 0.04
short	$1.7 \pm 0.7 \times 10^{5}$	5900 ± 2400	-7.1 ± 0.1	5.0 ± 0.7	12.1 ± 0.7	-0.34 ± 0.03

[a] All experiments were performed at 25 °C in 20 mM Hepes, pH 7.15, 100 mM NaCl, and 2 mM $CaCl_2$. [b] Errors represent the standard deviation of multiple experiments. [c] Uncertainty calculated by standard error propagation. [d] Uncertainty represents the 95% confidence interval to the linear best fit to the ΔH versus temperature data.

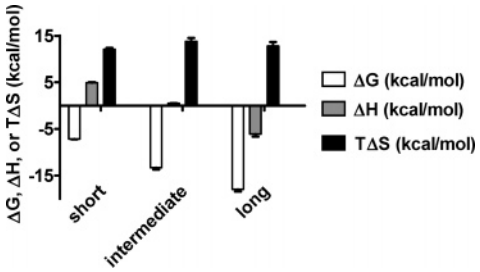

FIGURE 5: Thermodynamic parameters for CaM binding to CaMKII peptides. Shown are ΔG (white bars), ΔH (gray bars), and $T\Delta S$ (black bars) for the short, intermediate, and long peptides. All values are expressed in kcal/mol. Error bars represent the standard deviation of multiple experiments or were calculated using standard error propagation. Values were determined in 20 mM Hepes, pH 7.15, 100 mM NaCl, and 2 mM $CaCl_2$ at 25 °C.

generally cluster into two groups: those with ΔC_p near -0.76 kcal mol^{-1} deg^{-1} and those with ΔC_p near -0.38 kcal mol^{-1} deg^{-1} (*30*). Evidence was presented that peptides with ΔC_p near -0.38 kcal mol^{-1} deg^{-1} engage only a single lobe of CaM while those with ΔC_p near -0.76 kcal mol^{-1} deg^{-1} engage both lobes (*30*). The ΔC_p data presented here fit this trend in that the long and intermediate peptides group near -0.76 kcal mol^{-1} deg^{-1} while the short peptide groups near -0.38 kcal mol^{-1} deg^{-1}. On the basis of these findings, CaM appears to adopt a compact conformation, engaging the peptide using both lobes, when bound not only to the long peptide but also to the intermediate peptide. In contrast, the short peptide appears to engage with CaM in an extended conformation, binding via a single lobe.

If CaM buries similar surface area upon binding the long and intermediate peptides, how is 2500-fold greater potency obtained? The thermodynamic parameters (Table 5) indicate that ΔH distinguishes binding of these peptides, suggesting that more efficient hydrogen bonding and van der Waals contacts provide greater potency. Together, the ΔC_p and ΔH data support a model where CaM engages the intermediate peptide with both lobes but does not adopt a fully compact conformation because critical interactions at the N-terminus of the peptide are absent. Mutagenesis studies with full-length CaMKII using either alanine (*14*) or tryptophan substitutions (*15*) corroborate the idea that interactions between CaM and Phe 293 and Asn 294 of CaMKII are weak and/or absent when CaM interacts with unphosphorylated CaMKII but become important following phosphorylation. Furthermore, experiments using FRET with a dual-labeled fluorescent CaM support the notion that CaM adopts a semicompact conformation upon binding unphosphorylated CaMKII, which becomes fully compact after autophosphorylation (*17*, *31*). Hence, together with studies of the full-length CaMKII, the findings presented here suggest that when CaM is presented with the opportunity to engage residues 291−295 of CaMKII, it undergoes a modest conformational rearrangement that causes efficient interaction with Phe 293 and Asn 294 of CaMKII and hence very high affinity binding.

In addition to Phe 293 and Asn 294, the stretch of mostly positively charged residues encompassing Arg 296, Arg 297, Lys 298, and Leu 299 is also central to CaM binding to CaMKII. In this work, we observed that truncation of these residues caused a 30000-fold loss in binding (Table 5). The importance of these residues was also previously observed using alanine mutagenesis (*13*). The electrostatic interactions formed by these residues might be expected to primarily contribute to binding through a favorable $T\Delta S$ component. However, while $T\Delta S$ was more favorable for the intermediate peptide compared to the short peptide by 1.7 kcal/mol (Table 5), the primary thermodynamic difference between these peptides arose from ΔH. This suggests that other factors (hydrogen bonds and van der Waals contacts) also contribute to the more favorable binding of the intermediate peptide compared to the short peptide.

A molecular model of the different conformations of CaM when bound to both CaMKII-based peptides and CaMKII itself is presented in Figure 6. This model was constructed from crystallographic work (*23*, *32*, *33*), data presented here, and several previous studies including those described above (*12*−*15*, *17*, *31*, *33*, *34*). Unliganded Ca^{2+}-bound CaM is known to exist in an extended conformation (Figure 6A). Upon binding the short peptide, CaM appears to engage the target via only a single lobe (Figure 6B). In contrast, the intermediate peptide appears to bind CaM via both lobes (Figure 6C). The presence of CaMKII residues 291−295 in the long peptide allows CaM to occupy its optimal, high-affinity conformation (Figure 6D). Much data suggest that the different conformations of CaM when bound to these different CaMKII-based peptides correspond to conformations seen when CaM binds full-length CaMKII (Figure 6E−H). The crystal structure of CaMKII demonstrates that the CaM-binding motif is part of an autoinhibitory sequence that blocks the CaMKII active site (Figure 6E); in this structure, this autoinhibitory domain actually forms a coiled-coil interaction with a neighboring kinase domain (which is not depicted in Figure 6E). Initial CaM binding to CaMKII appears to occur via a single lobe of CaM (Figure 6F); this is sufficient to activate the enzyme but does not appear to displace the full autoinhibitory sequence away from CaMKII, and hence binding occurs with modest affinity. Binding of nucleotide to the ATP site is known to increase CaM affinity and at least partially allow engagement of both lobes of CaM with the target sequence; however, nucleotide binding does not appear to result in full disengagement of Phe 293 from the kinase domain to allow interaction with CaM (Figure 6G). Only after Thr 286 autophosphorylation does CaM fully disengage the autoinhibitory sequence from the kinase

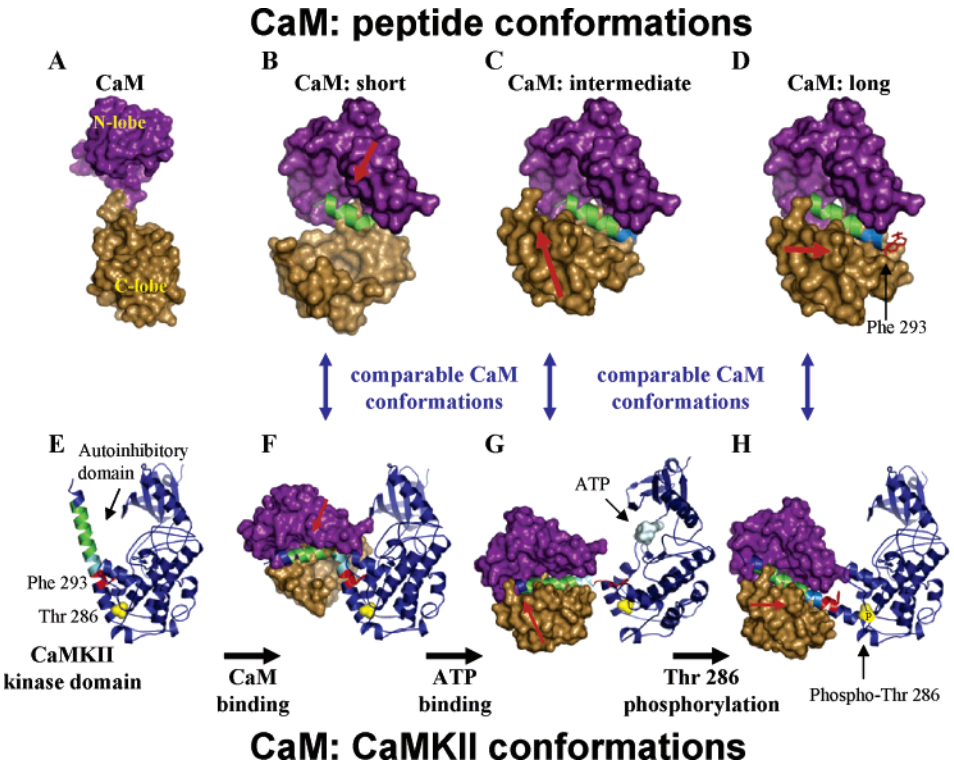

FIGURE 6: Molecular models of the different conformations of Ca^{2+}/CaM. Shown are models of unliganded Ca^{2+}/CaM (A) and Ca^{2+}/CaM bound to the short (B), intermediate (C), and long (D) peptides. Also shown are models of CaMKII (E), the initial Ca^{2+}/CaM−CaMKII complex (F), the Ca^{2+}/CaM−CaMKII complex with bound nucleotide in the ATP site (G), and the Ca^{2+}/CaM−CaMKII complex with Thr 286 phosphorylated (H). Data suggest that Ca^{2+}/CaM adopts a similar conformation when bound to the short peptide and when first binding to CaMKII [see (B) and (F)], when binding to the intermediate peptide and when binding to CaMKII in the presence of nucleotide [see (C) and (G)], and when binding to the long peptide and binding to Thr 286 phosphorylated CaMKII [see (D) and (H)]. In these models, the CaMKII-based peptide is depicted in a ribbon diagram with residues 293−295, 296−299, and 300−310 colored red, blue, and green, respectively. The conformational transitions that occur in Ca^{2+}/CaM are depicted with red arrows. (A), (D), and (E) are derived directly from X-ray structures (*23*, *32*, *33*), (B) and (C) are based on the Ca^{2+}/CaM−long peptide structure but modified on the basis of thermodynamic data, and (F), (G), and (H) are modeled on the basis of biochemical and structural data. Models and images were created using PyMol (*53*).

domain and adopt the high-affinity, "CaM trapped" conformation (Figure 6H).

The model of CaM trapping shown in Figure 6 suggests that CaM can adopt many different conformations when bound to both CaMKII and CaMKII-based peptides. Crystallography and NMR studies support the idea that CaM can adopt multiple conformations (*23*). For instance, Ca^{2+}/CaM was initially observed to interact with peptides in two binding modes that were classified as either 1-8-14 or 1-5-10 based on which residues in the target bury into the hydrophobic pockets in CaM (*35*). The long peptide was found to adopt a 1-5-10 binding mode (*35*). Recently, CaM has been observed to demonstrate far greater conformational flexibility upon binding to targets than had been previously anticipated (*16*, *36*). For instance, CaM binds to certain targets in an extended rather than collapsed fashion (*37*, *38*), in a parallel rather than antiparallel conformation (*39*), via only a single lobe instead of via both lobes (*40*), via binding a myristoyl moiety of the target rather than a peptide sequence (*41*), and via dimerization of two different CaM molecules (*42*).

In order to ascertain the affinity of the long and intermediate peptides, we employed a competition strategy where binding of potent peptides was studied in the presence of weaker peptides of known K_d. While not yet widely utilized, this approach has been applied in other systems to measure both very weak and very strong interactions and is particularly useful in conjunction with ITC where the range of K_d values that can be determined directly is small. For instance, competitive binding with ITC has been previously used to characterize weak interactions such as binding of protein tyrosine phosphatase 1B binding to inhibitors (*43*) and the Src SH2 domain to a dephosphorylated peptide (*44*); very potent interactions such as acarbose−glucoamylase (*45*), parvalbumin−cation (*46*), and HIV-1 protease−inhibitor (*47*, *48*) interactions have also been examined using competitive calorimetric approaches. Competitive binding has also proven useful for measuring the strength of CaM binding to peptides based on CaM kinase I (CaMKI) using fluorescence methods (*49*). While binding constants of ~1 pM have been measured for both CaM−CaMKI peptide and HIV-1 protease−inhibitor interactions, to our knowledge the K_d for the CaM−long peptide interaction of 0.07 ± 0.04 pM is the most potent yet measured using competition methods.

In this work, we observed a linear relationship between ΔH and temperature between 5 and 37 °C for all peptides. This result contrasts with a nonlinear ΔH versus temperature plot previously observed for CaM binding to the smMLCK peptide (*27*). For smMLCK, nonlinearity was attributed to the unfolding of the central helix of CaM above 25 °C, resulting in multiple CaM conformations in solution (*27*). It is known that multiple protein conformations can potentially lead to nonlinear plots of ΔH versus temperature; this has also been observed in the binding of the tandem SH2 domain of the Syk kinase to a dually phosphorylated ITAM peptide (*50*, *51*). However, our results indicate that the temperature-induced unfolding of the CaM central helix has surprisingly

little effect on the ΔH versus temperature relationship for CaM binding to CaMKII peptides. It may be that the ΔH of binding for the folded and partially unfolded conformation of CaM are similar, which would mask the presence of multiple CaM conformations above 25 °C.

The experiments presented here, together with other studies of CaM trapping employing both peptides and full-length CaMKII, have begun to uncover the molecular basis for CaM trapping. Future studies employing versions of CaM that contain only the N-terminal or C-terminal domain might provide further information into the conformations adopted by CaM when bound to CaMKII-based targets. However, a key question regarding CaM trapping that remains to be fully answered is its precise biological function. In this regard, CaM trapping has been proposed to impact the availability of CaM within the cell and hence impact the flow of information through Ca^{2+}-mediated signaling networks (*10*, *11*, *52*). CaM trapping is also believed to help to regulate the decoding of Ca^{2+}-spike frequency (*9*). Previously identified mutants of CaMKII shown to be deficient in CaM trapping could be useful in providing further information on the biological significance of CaMKII (*14*). Specifically, incorporation of these variants in genetically altered mice could yield new insights into the biological effects of CaM trapping. Combined with the thermodynamic characterization of CaM trapping described here, these studies would provide a better understanding of the role of CaM trapping in Ca^{2+}-mediated signaling processes.

ACKNOWLEDGMENT

We acknowledge Ago Ahene, Douglas Clark, and Holger Pils for use of the titration calorimeter, Wajiha Khan and Waleed Danho for peptide synthesis, Andy Hudmon for the CaM expression construct and aid in CaM purification, David Swinney and Richard Grucza for critical reading of the manuscript and useful discussion, and William Overall for helpful insights.

APPENDIX

In this section, the equations describing how the association constant and enthalpy of a tight binding interaction vary with the concentration of a competing ligand are derived. Shown in eq 7 is a linkage scheme for the competitive binding of two peptides (P_H and P_L) to the protein CaM.

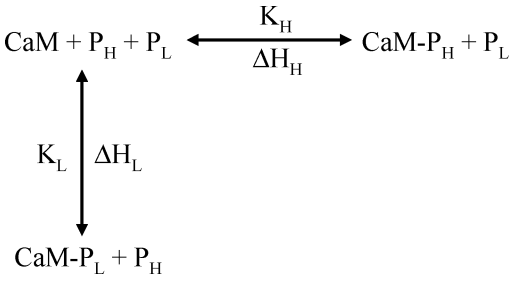

(7)

In this scheme, K_H and ΔH_H are the intrinsic association constant and enthalpy for binding of a high-affinity peptide, P_H; K_L and ΔH_L are the intrinsic association constant and enthalpy for binding of a lower affinity peptide, P_L.

To begin the derivation, the binding of P_H to CaM is chosen as the reference state. From simple linkage theory, the observed association constant (K_{obs}) for binding of P_H to CaM in the presence of P_L can be expressed as K_H divided by the subpartition function (Z_f) for binding of P_L to free CaM:

$$K_{obs} = K_H/Z_f \tag{8}$$

From linkage theory, Z_f is given as the following function of K_L and the concentration of P_L:

$$Z_f = 1 + K_L[P_L] \tag{9}$$

Substituting eq 9 into eq 8 gives

$$K_{obs} = K_H/(1 + K_L[P_L]) \tag{10}$$

This expression can be rearranged to give the association constant of interest, K_H, as a function of K_{obs}, K_L, and $[P_L]$:

$$K_H = K_{obs}(1 + K_L[P_L]) \tag{11}$$

Using this expression, the intrinsic association constant of the high-affinity peptide, K_H, can be calculated given an observed association constant, K_{obs}, an association constant for the low-affinity peptide, K_L, and the concentration of P_L.

An expression for ΔH_H, the intrinsic ΔH of the high-affinity peptide, can also be calculated from competition binding experiments if the enthalpy of the low-affinity peptide, ΔH_L, and an observed enthalpy of binding (ΔH_{obs}) are known. To derive this expression, the van't Hoff equation is employed:

$$\frac{\partial \ln K_{obs}}{\partial(1/T)} = -\frac{\Delta H_{obs}}{R} \tag{12}$$

In this expression, T is the temperature and R is the gas constant. Using the van't Hoff equation to differentiate eq 10 gives the expression:

$$\Delta H_{obs} = \Delta H_H - \frac{K_L[P_L]}{1 + K_L[P_L]}\Delta H_L \tag{13}$$

Under the conditions used in this study, $K_L[P_L] \gg 1$, so eq 13 simplifies to

$$\Delta H_{obs} \approx \Delta H_H - \Delta H_L \tag{14}$$

This can be rearranged to

$$\Delta H_H \approx \Delta H_{obs} + \Delta H_L \tag{15}$$

which gives the enthalpy of interest, ΔH_H, as a function of ΔH_{obs} and ΔH_L.

It should be noted that in the expressions above $[P_L]$ represents the free, not total, concentration of P_L. However, under the conditions used here $[P_L] \gg [CaM]$, indicating that

$$[P_L]_{free} \approx [P_L]_{total} \tag{16}$$

Hence, the total concentration of P_L can be used in eq 11 and eq 15 to calculate K_H and ΔH_H.

REFERENCES

1. Hudmon, A., and Schulman, H. (2002) Neuronal Ca^{2+}/calmodulin-dependent protein kinase II: The role of structure and autoregulation in cellular function, *Annu. Rev. Biochem. 71*, 473−510.

2. Griffith, L. C. (2004) Regulation of calcium/calmodulin-dependent protein kinase II activation by intramolecular and intermolecular interactions, *J. Neurosci. 24*, 8394−8398.
3. Colbran, R. J. (2004) Targeting of calcium/calmodulin-dependent protein kinase II, *Biochem. J. 378*, 1−16.
4. Yamauchi, T. (2005) Neuronal Ca^{2+}/calmodulin-dependent protein kinase II−discovery, progress in a quarter of a century, and perspective: implication for learning and memory, *Biol. Pharm. Bull. 28*, 1342−1354.
5. Merrill, M. A., Chen, Y., Strack, S., and Hell, J. W. (2005) Activity-driven postsynaptic translocation of CaMKII, *Trends Pharmacol. Sci.* 26, 645−653 (Epub 2005 Oct 25).
6. Soderling, T. R., Chang, B., and Brickey, D. (2001) Cellular signaling through multifunctional Ca^{2+}/calmodulin-dependent protein kinase II, *J. Biol. Chem. 276*, 3719−3722.
7. Saitoh, T., and Schwartz, J. H. (1985) Phosphorylation-dependent subcellular translocation of a Ca^{2+}/calmodulin-dependent protein kinase produces an autonomous enzyme in *Aplysia* neurons, *J. Cell Biol. 100*, 835−842.
8. Giese, K. P., Fedorov, N. B., Filipkowski, R. K., and Silva, A. J. (1998) Autophosphorylation at Thr286 of the α calcium-calmodulin kinase II in LTP and learning, *Science 279*, 870−873.
9. Meyer, T., Hanson, P. I., Stryer, L., and Schulman, H. (1992) Calmodulin trapping by calcium-calmodulin-dependent protein kinase, *Science 256*, 1199−1202.
10. Bhalla, U. S., and Iyengar, R. (1999) Emergent properties of networks of biological signaling pathways, *Science 283*, 381−387.
11. Holmes, W. R. (2000) Models of calmodulin trapping and CaM kinase II activation in a dendritic spine, *J. Comput. Neurosci. 8*, 65−85.
12. Putkey, J. A., and Waxham, M. N. (1996) A peptide model for calmodulin trapping by calcium/calmodulin-dependent protein kinase II, *J. Biol. Chem. 271*, 29619−29623.
13. Waxham, M. N., Tsai, A.-L., and Putkey, J. A. (1998) A mechanism for calmodulin (CaM) trapping by CaM-kinase II defined by a family of CaM-binding peptides, *J. Biol. Chem. 273*, 17579−17584.
14. Singla, S. I., Hudmon, A., Goldberg, J. M., Smith, J. L., and Schulman, H. (2001) Molecular characterization of calmodulin trapping by calcium/calmodulin-dependent protein kinase II, *J. Biol. Chem. 276*, 29353−29360.
15. Chin, D., and Means, A. R. (2002) Mechanisms for regulation of calmodulin kinase IIalpha by Ca(2+)/calmodulin and autophosphorylation of threonine 286, *Biochemistry 41*, 14001−14009.
16. Hoeflich, K. P., and Ikura, M. (2002) Calmodulin in action: diversity in target recognition and activation mechanisms, *Cell 108*, 739−742.
17. Morris, E. P., and Torok, K. (2001) Oligomeric structure of alpha-calmodulin-dependent protein kinase II, *J. Mol. Biol. 308*, 1−8.
18. Klee, C. B., and Vanaman, T. C. (1982) Calmodulin, *Adv. Protein Chem. 35*, 213−321.
19. Fukada, H., and Takahashi, K. (1998) Enthalpy and heat capacity changes for the proton dissociation of various buffer components in 0.1 M potassium chloride, *Proteins 33*, 159−166.
20. Sigurskjold, B. W. (2000) Exact analysis of competition ligand binding by displacement isothermal titration calorimetry, *Anal. Biochem. 277*, 260−266.
21. Fraczkiewicz, R., and Braun, W. (1998) Exact and efficient analytical calculation of the accessible surface areas and their gradients for macromolecules, *J. Comput. Chem. 19*, 319−333.
22. Babu, Y. S., Sack, J. S., Greenhough, T. J., Bugg, C. E., Means, A. R., and Cook, W. J. (1985) Three-dimensional structure of calmodulin, *Nature 315*, 37−40.
23. Meador, W. E., Means, A. R., and Quiocho, F. A. (1993) Modulation of calmodulin plasticity in molecular recognition on the basis of X-ray structures, *Science 262*, 1718.
24. Spolar, R. S., and Record, M. T., Jr. (1994) Coupling of local folding to site-specific binding of proteins to DNA, *Science 263*, 777−784.
25. Baker, B. M., and Murphy, K. P. (1997) Dissecting the energetics of a protein-protein interaction: the binding of ovomucoid third domain to elastase, *J. Mol. Biol. 268*, 557−569.
26. Bradshaw, J. M., and Waksman, G. (1998) Calorimetric investigation of proton linkage by monitoring both the enthalpy and association constant of binding: application to the interaction of the Src SH2 domain with a high-affinity tyrosyl phosphopeptide, *Biochemistry 37*, 15400−15407.
27. Wintrode, P. L., and Privalov, P. L. (1997) Energetics of target peptide recognition by calmodulin: a calorimetric study, *J. Mol. Biol. 266*, 1050−1062.
28. Murphy, K. P., and Freire, E. (1992) Thermodynamics of structural stability and cooperative folding behavior in proteins, *Adv. Protein Chem. 43*, 313−361.
29. Wiseman, T., Williston, S., Brandts, J. F., and Lin, L. N. (1989) Rapid measurement of binding constants and heats of binding using a new titration calorimeter, *Anal. Biochem. 179*, 131−137.
30. Brokx, R. D., Lopez, M. M., Vogel, H. J., and Makhatadze, G. I. (2001) Energetics of target peptide binding by calmodulin reveals different modes of binding, *J. Biol. Chem. 276*, 14083−14091 (Epub 2001 Jan 29).
31. Tzortzopoulos, A., and Torok, K. (2004) Mechanism of the T286A-mutant alphaCaMKII interactions with Ca^{2+}/calmodulin and ATP, *Biochemistry 43*, 6404−6414.
32. Chattopadhyaya, R., Meador, W. E., Means, A. R., and Quiocho, F. A. (1992) Calmodulin structure refined at 1.7 Å resolution, *J. Mol. Biol. 228*, 1177−1192.
33. Rosenberg, O. S., Deindl, S., Sung, R. J., Nairn, A. C., and Kuriyan, J. (2005) Structure of the autoinhibited kinase domain of CaMKII and SAXS analysis of the holoenzyme, *Cell 123*, 849−860.
34. Shifman, J. M., Choi, M. H., Mihalas, S., Mayo, S. L., and Kennedy, M. B. (2006) Ca^{2+}/calmodulin-dependent protein kinase II (CaMKII) is activated by calmodulin with two bound calciums, *Proc. Natl. Acad. Sci. U.S.A. 103*, 13968−13973 (Epub 2006 Sep 11).
35. Rhoads, A. R., and Friedberg, F. (1997) Sequence motifs for calmodulin recognition, *FASEB J. 11*, 331−340.
36. Vetter, S. W., and Leclerc, E. (2003) Novel aspects of calmodulin target recognition and activation, *Eur. J. Biochem. 270*, 404−414.
37. Schumacher, M. A., Rivard, A. F., Bachinger, H. P., and Adelman, J. P. (2001) Structure of the gating domain of a Ca^{2+}-activated K^+ channel complexed with Ca^{2+}/calmodulin, *Nature 410*, 1120−1124.
38. Drum, C. L., Yan, S. Z., Bard, J., Shen, Y. Q., Lu, D., Soelaiman, S., Grabarek, Z., Bohm, A., and Tang, W. J. (2002) Structural basis for the activation of anthrax adenylyl cyclase exotoxin by calmodulin, *Nature 415*, 396−402.
39. Osawa, M., Tokumitsu, H., Swindells, M. B., Kurihara, H., Orita, M., Shibanuma, T., Furuya, T., and Ikura, M. (1999) A novel target recognition revealed by calmodulin in complex with Ca^{2+}-calmodulin-dependent kinase kinase, *Nat. Struct. Biol. 6*, 819−824.
40. Elshorst, B., Hennig, M., Forsterling, H., Diener, A., Maurer, M., Schulte, P., Schwalbe, H., Griesinger, C., Krebs, J., Schmid, H., Vorherr, T., and Carafoli, E. (1999) NMR solution structure of a complex of calmodulin with a binding peptide of the Ca^{2+} pump, *Biochemistry 38*, 12320−12332.
41. Matsubara, M., Nakatsu, T., Kato, H., and Taniguchi, H. (2004) Crystal structure of a myristoylated CAP-23/NAP-22 N-terminal domain complexed with Ca^{2+}/calmodulin, *EMBO J. 23*, 712−718 (Epub 2004 Feb 12).
42. Ye, Q., Li, X., Wong, A., Wei, Q., and Jia, Z. (2006) Structure of calmodulin bound to a calcineurin peptide: a new way of making an old binding mode, *Biochemistry 45*, 738−745.
43. Zhang, Y. L., and Zhang, Z. Y. (1998) Low-affinity binding determined by titration calorimetry using a high-affinity coupling ligand: a thermodynamic study of ligand binding to protein tyrosine phosphatase 1B, *Anal. Biochem. 261*, 139−148.
44. Bradshaw, J. M., Mitaxov, V., and Waksman, G. (1999) Investigation of phosphotyrosine recognition by the SH2 domain of the Src kinase, *J. Mol. Biol. 293*, 971−985.
45. Sigurskjold, B. W., Berland, C. R., and Svensson, B. (1994) Thermodynamics of inhibitor binding to the catalytic site of glucoamylase from *Aspergillus niger* determined by displacement titration calorimetry, *Biochemistry 33*, 10191−10199.
46. Henzl, M. T., Larson, J. D., and Agah, S. (2003) Estimation of parvalbumin Ca(2+)- and Mg(2+)-binding constants by global least-squares analysis of isothermal titration calorimetry data, *Anal. Biochem. 319*, 216−233.
47. Velazquez-Campoy, A., Kiso, Y., and Freire, E. (2001) The binding energetics of first- and second-generation HIV-1 protease inhibitors: implications for drug design, *Arch. Biochem. Biophys. 390*, 169−175.

48. King, N. M., Prabu-Jeyabalan, M., Nalivaika, E. A., Wigerinck, P., de Bethune, M. P., and Schiffer, C. A. (2004) Structural and thermodynamic basis for the binding of TMC114, a next-generation human immunodeficiency virus type 1 protease inhibitor, *J. Virol. 78*, 12012−12021.
49. Clapperton, J. A., Martin, S. R., Smerdon, S. J., Gamblin, S. J., and Bayley, P. M. (2002) Structure of the complex of calmodulin with the target sequence of calmodulin-dependent protein kinase I: studies of the kinase activation mechanism, *Biochemistry 41*, 14669−14679.
50. Grucza, R. A., Futterer, K., Chan, A. C., and Waksman, G. (1999) Thermodynamic study of the binding of the tandem-SH2 domain of the Syk kinase to a dually phosphorylated ITAM peptide: evidence for two conformers, *Biochemistry 38*, 5024−5033.
51. Kumaran, S., Grucza, R. A., and Waksman, G. (2003) The tandem Src homology 2 domain of the Syk kinase: a molecular device that adapts to interphosphotyrosine distances, *Proc. Natl. Acad. Sci. U.S.A. 100*, 14828−33 (Epub 2003 Dec 1).
52. Schulman, H., and Hanson, P. I. (1993) Multifunctional Ca^{2+}/calmodulin-dependent protein kinase, *Neurochem. Res. 18*, 65−77.
53. DeLano, W. L. (2002) The PyMOL molecular graphics system, DeLano Scientific, San Carlos, CA.

BI700013Y